A single *Photorhabdus* gene, *makes caterpillars floppy* (*mcf*), allows *Escherichia coli* to persist within and kill insects

P. J. Daborn, N. Waterfield, C. P. Silva, C. P. Y. Au, S. Sharma, and R. H. ffrench-Constant*

Department of Biology and Biochemistry, University of Bath, Bath BA2 7AY, United Kingdom

Edited by John H. Law, University of Arizona, Tucson, AZ, and approved March 26, 2002 (received for review February 5, 2002)

***Photorhabdus luminescens*, a bacterium with alternate pathogenic and symbiotic phases of its lifestyle, represents a source of novel genes associated with both virulence and symbiosis. This entomopathogen lives in a ''symbiosis of pathogens'' with nematodes that invade insects. Thus the bacteria are symbiotic with entomopathogenic nematodes but become pathogenic on release from the nematode into the insect blood system. Within the insect, the bacteria need to both avoid the peptide- and cellular- (hemocyte) mediated immune response and also to kill the host, which then acts as a reservoir for bacterial and nematode reproduction. However, the mechanisms whereby *Photorhabdus* evades the insect immune system and kills the host are unclear. Here we show that a single large *Photorhabdus* gene, *makes caterpillars floppy* (*mcf*), is sufficient to allow *Esherichia coli* both to persist within and kill an insect. The predicted high molecular weight Mcf toxin has little similarity to other known protein sequences but carries a BH3 domain and triggers apoptosis in both insect hemocytes and the midgut epithelium.**

insecticide | *Photorhabdus* | pathogenicity | apoptosis | toxin

Characterization of bacterial genomes involved in pathogenicity and symbiosis is important to define the patterns of gene acquisition or loss involved in the evolution of these traits (1–4). The bacterium *Photorhabdus luminescens* forms a model system in this context as it has both symbiotic and pathogenic phases of its lifecycle (5, 6). *P. luminescens* is also a member of the Enterobacteriaceae, facilitating comparison of putative virulence/symbiosis factors with well studied bacteria such as *Esherichia coli* (7). Previous genomic sample sequencing of *P. luminescens* subsp. *akhurstii* strain W14 identified numerous genes with homology either to known virulence factors from *P. luminescens*, such as the *toxin complex* (*tc*) genes (8) or to putative virulence factors identified in other pathogenic bacteria (7). However, 53% of the genes sampled are clearly distinct from those found in the genome of *E. coli* K12 (7), suggesting that the *P. luminescens* genome may contain a large number of novel genes involved either in pathogenicity, symbiosis, or both.

Photorhabdus luminescens has an unusual lifecycle in which it spends part of the time in an apparently symbiotic, or benign, relationship in the gut of entomopathogenic nematodes from the family Heterorhabditidae (6) and part of the time killing and bioconverting the insect host which the nematode partner penetrates (5, 9). In this lifecycle, *P. luminescens* needs to be able to both kill its insect host and also to persist within the gut of its nematode carrier. This bi-phasic lifestyle presumably involves a switch between an insect-pathogenic and a nematode-symbiotic state. Several anti-insect virulence factors have been identified or inferred from biochemical and genetic studies (5, 8, 9). However available sample sequence from the *P. luminescens* genome shows that this bacterium may carry a number of different anti-insect toxins (7, 10), inplying either that these multiple toxins act at different sites and/or with different modes of action, or that *P. luminescens* uses functional redundancy or ''overkill.'' Given that death of the insect host is critical to the successful release of new infective juvenile nematodes, which transmit the bacteria from host to host, this latter possibility is not unlikely.

To identify novel virulence factors in the *P. luminescens* genome, we have developed the tobacco hornworm caterpillar, *Manduca sexta*, as a model insect for bacterial infection (11). As an insect host, *M. sexta* has the advantages of both a large size and a well-studied insect immune system. We constructed a *P. luminescens* W14 cosmid library in *E. coli* and screened for insect virulence factors by injection of individual cosmids into *M. sexta* larvae. Normally, injection of wild-type *E. coli* into *M. sexta* results in rapid encapsulation of all of the bacteria by the insect hemocytes, completely clearing the infection from the hemocoel (11). These capsules, or nodules, are formed by complex interactions between different subpopulations of the hemocytes, which result in encapsulation of the bacteria and final melanization of the resulting capsule (12, 13). Once encapsulated the trapped bacteria subsequently die. Survival of *E. coli* within the insect hemocoel, in the face of an active immune system, is therefore unprecedented.

Here we report the isolation of a 33-kb *P. luminescens* cosmid that not only allows *E. coli* to persist within the insect but also results in a characteristic loss of body turgor followed by insect death. Insertional mutagenesis of the cosmid shows that a single, 8.8-kb gene, *makes caterpillars floppy* (*mcf*), is associated both with bacterial persistence in the host and also insect death. The amino acid sequence predicted by *mcf* shows only partial homology to known proteins; however, it does carry a BH3 domain, a domain found in pro-apoptotic proteins (14). The Mcf toxin appears to cause apoptosis in both the insect hemocytes and the insect midgut epithelium. The potential use of toxins active on both the midgut and the insect immune system is discussed.

Materials and Methods

Strains and Library Preparation. The cosmid library was prepared from *P. luminescens* subsp. *akhurstii* strain W14 genomic DNA by MWG Biotech (Munich). DNA was physically sheared, size selected for fragments of ≈30 kb, and then cloned into pWEB. The average insert size (≈32 kb) was determined by restriction analysis of a random selection of clones. For Southern analysis of *mcf* homologs, three other strains were used: *P. luminescens* subsp. *temperata* strain K122, *P. luminescens* subsp. *laumondii* strain TTO1, and *P. asymbiotica* [a new species recently split from *P. luminescens* (15)] strain ATCC43949. The first two strains were isolated from their nematode symbionts from Ireland and Trinidad, respectively. The third strain was isolated

This paper was submitted directly (Track II) to the PNAS office.

Abbreviations: GIM, Graces insect medium; TUNEL, terminal deoxynucleotidyltransferase-mediated UTP end labeling; GFP, green fluorescent protein.

Data deposition: The sequence reported in this paper has been deposited in the GenBank database (accession no. AF503504).

*To whom reprint requests should be addressed. E-mail: bssrfc@bath.ac.uk.

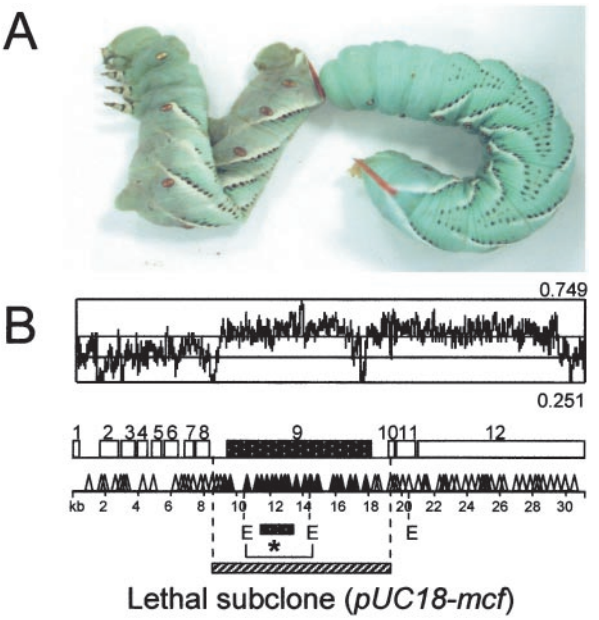

Fig. 1. The *mcf* gene causes loss of insect body turgor and is encoded within a putative pathogenicity island. (*A*) Fifth instar *M. sexta* larvae 24 h after injection of 2×10^6 *E. coli* cells containing H3 cosmid (left) and 2×10^6 *E. coli* cells without H3 cosmid (right). Note the loss of body turgor, or floppy phenotype, in the caterpillar on the left. (*B*) Genomic location and insertional mutagenesis of the H3 cosmid. The 33 kb of the H3 cosmid predicts 12 ORFs (ORF numbers above open boxes). Transposon mutagenesis shows location of transposons removing floppy and lethal phenotypes (▲) or leaving both phenotypes intact (△). The cluster of transposons that remove both phenotypes all lie within ORF nine, termed *mcf*. The relative location of a subclone containing only the *mcf* ORF is shown (E = *Eco*RI restriction sites). The shift in GC content (from 0.41 for the genome to 0.53 for the whole cosmid) across the region suggests that *mcf* lies within a pathogenicity island (see text). *, Probe used in the Southern analysis (see Fig. 2).

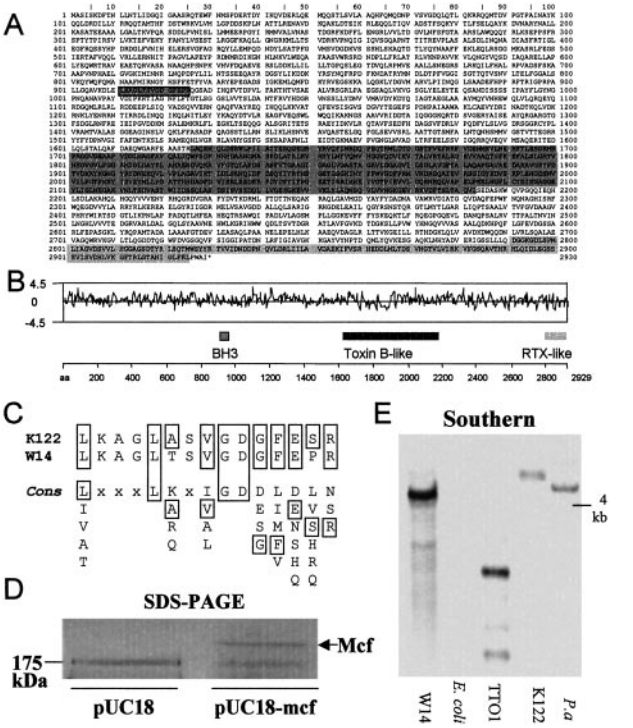

Fig. 2. The *mcf* gene predicts a novel toxin of high molecular weight. (*A*) Predicted amino acid sequence of the Mcf protein. The three shaded regions show regions of homology to other known proteins (see text). (*B*) Relative locations of the three regions of homology in relation to a Kyte-Doolittle hydrophilicity plot of the predicted protein. Note that the region homologous to the translocation domain of Toxin B is predominantly hydrophobic. (*C*) Match to the BH3 domain consensus sequence for Mcf toxins from two different *Photorhabdus* strains, W14 and K122. The consensus sequence for the BH3 motif is shown below. (*D*) SDS/PAGE gel of cytosolic fraction of Mcf expressing *E. coli*. An arrow indicates the presence of the Mcf protein (predicted weight of 324 kDa), which migrates at a higher molecular weight than the 174-kDa marker. (*E*) Southern blot of genomic DNA cut with *Eco*RI from four different *Photorhabdus* strains and *E. coli* probed with a fragment of *mcf* (see Fig. 1*B* for location of probe used). Note that the *mcf* DNA probe hybridizes at high stringency to all of the *Photorhabdus* strains but not *E. coli* (see text). Key to species and subspecies: *P. luminescens* subsp. *akhurstii* W14 (W14). *P. luminescens* subsp. *laumondii* TT 01(TT01), *P. luminescens* strain K122, which is probably subsp. *temperata* based on a description of its nematode host (K122), and *P. asymbiotica* ATCC43949 (*P.a*).

from a human wound, in the apparent absence of any potential nematode partner.

Insect Injection and Library Screening. The W14 cosmid library was arrayed into 96-well microtitre plates. For injection, individual clones were grown at 37°C overnight in 1 ml of LB with shaking. Ten microliters ($\approx 2 \times 10^7$ recombinant *E. coli* cells) of each bacterial culture was then injected into the hemocoel of individual fifth instar *M. sexta*. Injected larvae were scored for mortality after 48 h, in reference to control larvae injected with *E. coli* alone. In the first screen, injected larvae were examined at 24 and 48 h after injection. Clones showing insect mortality were rescreened three times, by injecting three individual larvae per clone, to look for a repeatable effect. Animals injected with positive clones also were examined for changes in appearance before death, such as changes in color or body turgor.

Cosmid Mutagenesis, Sequencing, and Southern Analysis. To ascertain which ORF within an individual cosmid was associated with the positive phenotype, we used insertional mutagenesis with a EZ::TN<TET1> transposon (Epicentre). Transposon mutants of individual cosmids were then re-screened to look for loss or retention of the phenotype (in this case loss of body turgor and death). Transposon mutants also were used as entry points in nucleotide sequencing of the positive H3 cosmid. This enabled us to ascribe loss of a specific phenotype to a specific gene. Cosmid DNA was prepared on a RoboPrep plasmid preparation robot (MWG Biotech) and sequenced on an ABI3700 nucleotide sequencer (Applied Biosystems). Sequences were assembled by using the LASERGENE software package (DNASTAR, Madison, WI). Southern analysis of *mcf* homologs in different *Photorhabdus* strains was performed by using a 4-kb *Eco*RI restriction fragment (Fig. 1) from W14 *mcf*.

Insect Histopathology and Hemocytes. For insect histopathology, whole larvae were fixed overnight in Bouin's solution (Sigma), after several incisions had been made in the cuticle to allow the fixative to permeate the cadaver. Larvae were then embedded in paraffin by using a Leica TP1020 automatic tissue processor. Sections were cut at 3–5 μm, stained with hematoxylin/eosin, and mounted on glass slides with DePeX-mounting medium. For terminal deoxynucleotidyltransferase-mediated UTP end labeling (TUNEL) straining, similar larval sections were fixed in 4% paraformaldehyde in PBS and embedded in paraffin as described previously, using the TUNEL method according to the manufacturer instructions (*in situ* cell death detection kit, Roche Molecular Biochemical).

Hemocyte Monolayers. *M. sexta* larvae were selected 1 d after ecdysis to the fifth larval stage (instar). Insects were chilled on

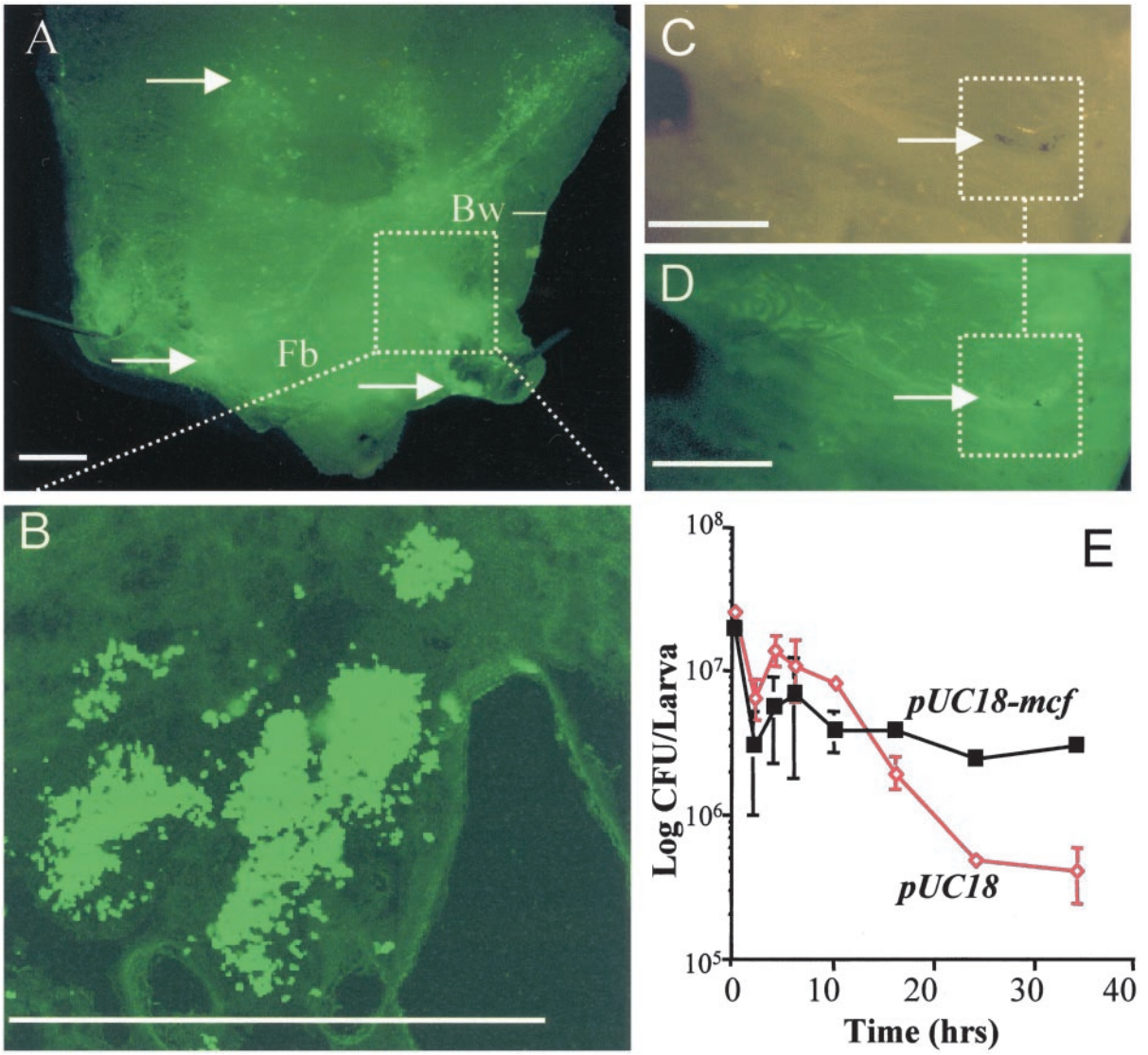

Fig. 3. GFP expressing *E. coli* carrying the *mcf* encoding subclone (*pUC18-mcf*) can persist within the insect model *M. sexta*. (*A*) Dissection of posterior of fifth instar larvae of *M. sexta* 16 h after injection of *pUC18-mcf*. Note the aggregations of GFP expressing bacteria within the fat body (Fb) and body wall (Bw) of the caterpillar. (*B*) High magnification of GFP-expressing bacterial clusters confirm that they consist of clumps of individual recombinant *E. coli*. (*C* and *D*) Parallel low magnification views of bacterial aggregations viewed under light and GFP-enhanced microscopy. Note how one of the bacterial aggregations (*C*) has been encapsulated by the insect hemocytes and brown melanin (arrow) deposited. A GFP enhanced view (*D*) of the same aggregations (arrows) shows the presence of GFP expressing and *pUC18-mcf* carrying *E. coli*. (Scale bar = 0.2 cm in *A–E*.) (*E*) Numbers of recoverable bacteria persisting over time in *M. sexta*. Note that *E. coli* carrying *pUC18-mcf* persist longer in an infected insect than *E. coli* carrying the *pUC18* vector alone. *E. coli* carrying *pUC18* alone were encapsulated as expected (data not shown).

ice for 30 min and swabbed with 70% ethanol before bleeding from the cut dorsal horn. Approximately 100 μl of hemolymph was allowed to drip into 900 μl of ice-cold Graces insect medium (GIM, Sigma) in a microcentrifuge tube. Hemocyte density was adjusted to $\approx 5 \times 10^6$ ml^{-1} in GIM by using a hemocytometer. Coverslips (10 mm) were washed in 70% ethanol and placed centrally into each well of a 24-well plate. The cell suspension (100 μl) was pipetted onto each coverslip and then left undisturbed for 60 min (room temperature) to allow the hemocytes to settle and form a monolayer. The monolayer was washed gently with a few drops of GIM and removed to a new well containing 400 μl of fresh GIM. Monolayers incubated with cytosolic fractions of Mcf expressing *E. coli* diluted 1:10 in GIM. For differential interference contrast microscopy imaging, a X40 Fluor water immersion lens was used on an upright Nikon E1000 microscope. Images were collected at 3-min intervals for 6 h with a Hamamatsu C4880–07 camera controlled by using METAMORPH software (Universal Imaging, Media, PA).

Results and Discussion

P. luminescens appears to encode numerous putative (7) and proven (8, 10) toxins in its genome. Although we understand the histopathological effects of some of these insecticidal toxins, such as the gut active Toxin complex A (16), we do not understand the role of specific toxins in insect death. To look for toxins capable of killing insects when expressed in recombinant *E. coli*, we screened a W14 cosmid library. After injection of 300 individual clones, we isolated a single cosmid (termed H3), which not only allows its *E. coli* host to persist within but also to kill its insect host. Injection of *E. coli* containing the H3 cosmid results in a rapid (within 12 h) loss of caterpillar body turgor (Fig. 1*A*) and death of the larvae (time of death, 24.1 h $\pm$ SE of 3.25). We

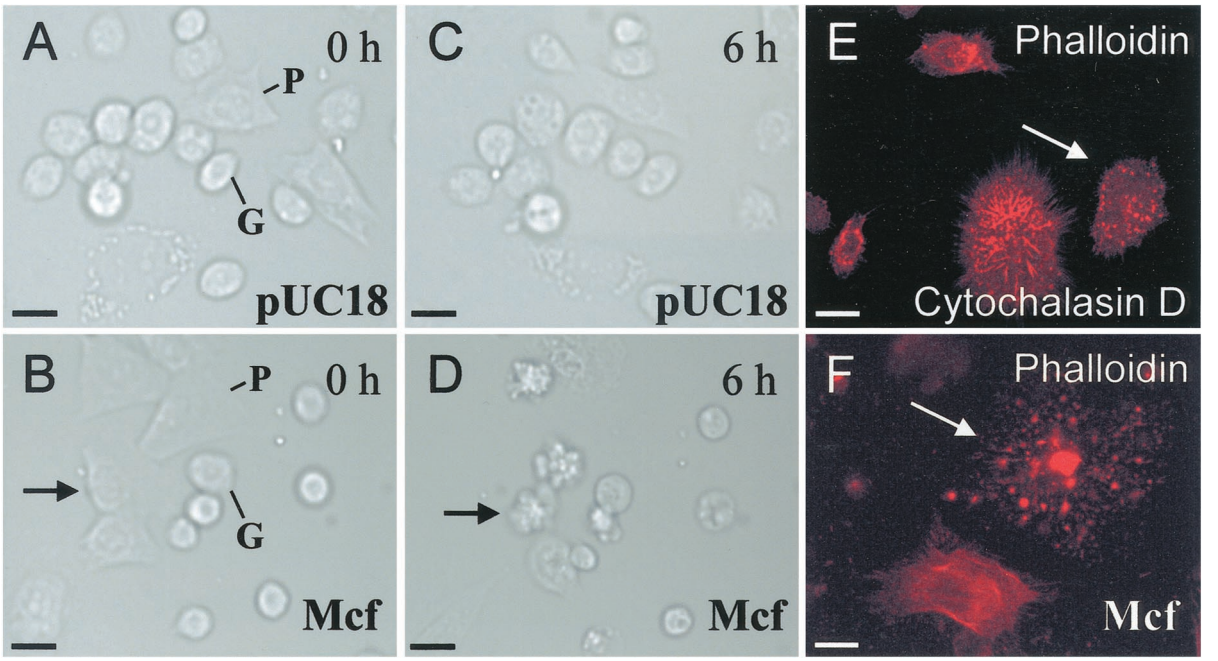

Fig. 4. Hemocyte monolayers show that Mcf toxin acts on insect blood cells within 6 h by disrupting the cytoskeleton. (*A* and *B*) Hemocyte monolayers treated with cytosolic fractions of either *pUC18* or *pUC18-mcf* carrying *E. coli* at the start of time-lapse differential interference contrast microscopy imaging. (*C* and *D*) The same preparations 6 h after treatment. Note that the plasmatocyte (P) indicated by an arrow (*D*) has begun to disintegrate by producing a series of rounded blebs. Note that the cell highlighted by an arrow is the same cell (*B* and *D*). Taken together with observations from TUNEL staining, the blebbing phenotype associated with Mcf-mediated hemocyte death is strongly supportive of programmed cell death. The full time lapse series of Mcf toxin action can be viewed at www.bath.ac.uk/bio-sci/quicktime.htm. (*E* and *F*) FITC-phalloidin staining of hemocyte monolayers treated either with cytochalasin D or Mcf. Note that treatment with both toxins disintegrates the actin cytoskeleton leaving a punctate staining pattern of residual actin. (Scale bar = 10 μm.)

termed this loss of body turgor the "floppy" phenotype. Insertional mutagenesis of this cosmid (Fig. 1*B*) shows that a single ORF, termed *mcf*, is responsible for these phenotypes. Inserted transposons also were used as entry points for sequencing of the entire cosmid. This dual approach allowed us both to derive nucleotide sequence of the entire 33-kb cosmid and to attribute phenotype loss to a specific gene. Sequencing of the cosmid was completed from 126 transposon entry points, 39 of which negated both floppy and lethal phenotypes. All of the 39 insertions associated with phenotype loss lie within the 8.8-kb predicted ORF of *mcf* (Fig. 1*B*). To confirm the hypothesis that *mcf* causes both the floppy and lethal phenotypes associated with the complete cosmid, we subcloned the *mcf* gene alone (Fig. 1*B*). This subclone also confers the same ability on *E. coli* to both render caterpillars floppy and to kill them within an equivalent space of time (data not shown).

The *mcf* ORF predicts a high molecular weight protein of 2,929 aa (Fig. 2*A*) with a molecular weight of 324 kDa and PI of 5.4. Searches of current databases reveal three areas of similarity with known proteins (Fig. 2*B*). First, Mcf contains a consensus sequence for a BH3 domain (Fig. 2*C*). Proteins involved in apoptosis that contain only this domain are pro-apoptotic (14). Second, residues 1,626–2,139 show 20% identity to residues 873–1,362 from *Clostridium difficile* toxin B. This region lies within part of toxin B thought to be involved in translocation (17). Finally, the predicted C terminus of Mcf contains a region (residues 2,791–2,925) that shows similarity to a repeated sequence in the C terminus of *apxIVA*, an RTX-like toxin from *Actinobacillus pleuropneumoniae* (18). The remainder of the predicted protein shows no significant homology to known proteins and little variation in predicted hydrophobicity (Fig. 2*B*). SDS/PAGE analysis of cytosolic preparations of *mcf* encoding recombinant *E. coli* reveal the presence of a single protein of the predicted molecular weight (Fig. 2*D*). These preparations are highly toxic to caterpillars on injection (data not shown). Southern analysis of three other *P. luminescens* strains (Fig. 2*E*) suggests that homologs of *mcf* are carried by other *Photorhabdus* strains, which would be consistent with the presence of the toxin being required for death of the insect host.

The complete nucleotide sequence of the H3 cosmid (GenBank accession no. AF503504) encompasses 33 kb of genomic DNA and contains 12 predicted ORFs (Fig. 1*B*). The similarity of the surrounding predicted gene products with other putative virulence factors and the shift in GC content (Fig. 1*B*) associated with the genomic location of *mcf* suggests that this region constitutes a pathogenicity island. Thus, upstream of *mcf* is an ORF (orf 4), which shows similarity to *dlpA* or *dotA* of *Legionella pneumophila* (19). The *dot/icm* system encodes a type IV secretion system related to the *Shigella flexneri* Col1b Inc1 plasmid (19). Within this system, DotA encodes a cytoplasmic membrane protein required for macrophage cell killing by *L. pneumophila* (20). Downstream of *mcf* lie two ORFs (orfs 11 and 12), which predict proteins with similarity to the HecA and HecB hemolysins also found in a wide range of other Enterobacteriaceae. The presence of these macrophage killing and hemolysin-like genes suggests that this pathogenicity island may encode several genes involved in overcoming host blood cells.

To investigate how *E. coli* carrying the *mcf* containing *pUC18* plasmid (*pUC18-mcf*) can persist within *M. sexta*, we labeled *pUC18-mcf* with a second plasmid (*pBBR2*) expressing green fluorescent protein (GFP). We then injected caterpillars with the marked *pUC18-mcf* and dissected caterpillars at different time intervals postinjection to look for *E. coli* expressing GFP. Dissection of *Manduca* infected with the GFP expressing *mcf E. coli* showed visible aggregations of bacteria persisting within insect tissues (Fig. 3 *A* and *B*). Quantitation of bacterial persistence over time (Fig. 3*E*) shows that *pUC18-mcf* containing *E. coli* can persist longer in the presence of the insect immune

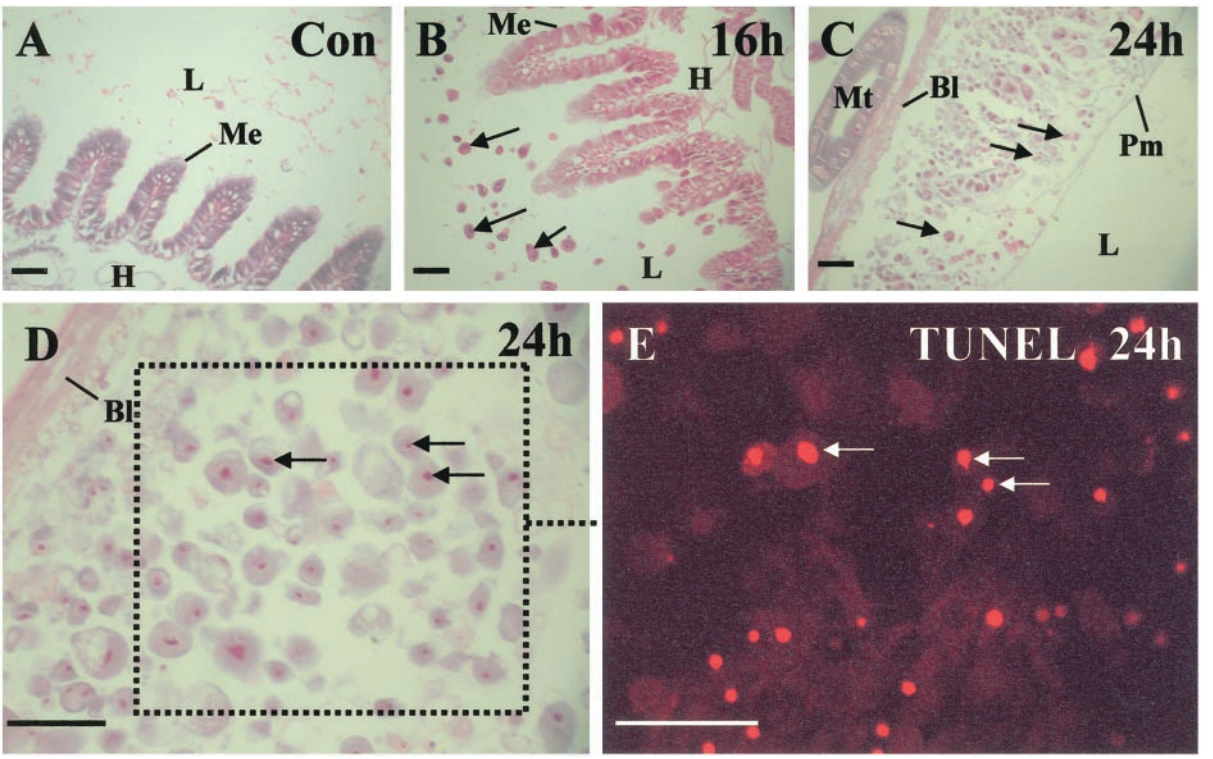

Fig. 5. *M. sexta* infected with Mcf encoding *E. coli* show massive destruction of the midgut epithelium. (*A*) Light microscopy of a stained control section of *M. sexta* fourth instar midgut. Note the midgut epithelium (Me), which separates the lumen (L) of the gut from the insect hemocoel (H). (*B*) Section of midgut 16 h after infection with *pUC18-mcf E. coli*. The cells of the midgut have begun to bleb into the gut lumen (arrows). (*C*) Section of midgut 24 h after infection. The midgut epithelium has disintegrated leaving the space between the basal lamina (Bl) and the peritrophic membrane (Pm) packed with blebbed cells. (*D*) Detail of disintegrated epithelium showing that nuceli within the cellular blebs are pycnotic and often surrounded by vacuoles. (*E*) TUNEL staining of disintegrated epithelium suggesting that the cells are undergoing apoptosis. (Scale bar = 100 μm.)

system than *E. coli* containing *pUC18* plasmid alone. *E. coli* carrying *pUC18* alone were encapsulated at high frequency as previously documented by others (21). Detailed examination of the bacterial aggregations often shows partial encapsulation and melanization of the bacteria (Fig. 3 *C* and *D*). These observations suggest that although the Mcf expressing *E. coli* are recognized by the hemocytes, they cannot be successfully encapsulated. Such a phenotype could be caused by the direct toxicity of expressed Mcf on hemocytes attempting to adhere to and encapsulate the bacteria or by interference with the melanization cascade.

To test the effect of Mcf on hemocytes, we added preparations of Mcf protein to hemocyte monolayers and examined them under differential interference contrast microscopy illumination and time-lapse photography (Fig. 4). In the presence of cytosolic fractions from *E. coli* carrying *pUC18* alone, hemocytes exhibit normal motility and can persist for at least 12 h as a monolayer with no visible adverse effects (Fig. 4 *A* and *C*). Granulocytes show limited motility whereas the more amoeboid plasmatocytes move freely across the monolayer (www.bath.ac.uk/bio-sci/quicktime.htm). In the presence of all fractions containing Mcf, both cell types show marked changes in morphology within 6 h and affected cells begin to disintegrate by producing numerous circular blebs (Fig. 4*E*). This phenotype is similar to that observed in other cell types undergoing apoptosis (22). Taken together with the observations from TUNEL staining, the blebbing phenotype associated with Mcf-mediated hemocyte death is consistent with Mcf triggering programmed cell death. Actin straining of Mcf-treated cells shows that the cytoskeleton has disintegrated, remaining only as a series of highly staining foci (Fig. 4*F*). We note that this final actin staining pattern is similar to that achieved by treatment of hemocytes with the fungal toxin cytochalasin D (Fig. 4*E*) (23).

Finally, to examine the potential cause of the rapid loss of body turgor associated with the floppy phenotype, we examined the histopathology of insect hosts infected with *mcf* containing *E. coli*. Sections of infected larvae were stained and examined via light microscopy (Fig. 5 *A–D*). Given that both the insect midgut and the malpighian tubules are associated with osmoregulation of the insect hemolymph, disruption of either of which could cause the floppy phenotype, we examined the histopathology of these structures in detail. The malpighian tubules (approximating in function to vertebrate kidneys) appear unaffected before the time of insect death, whereas the midgut epithelium is severely affected as early as 12 h. The midgut epithelium is a simple epithelium composed of two main cell types (columnar and goblet cells) and is fringed on the lumen side with a brush border membrane (Fig. 5*A*). After infection with *mcf* containing *E. coli*, the midgut epithelium begins to bleb into the lumen of the gut. Both goblet and columnar cells elongate and shed circular blebs often containing the cell nucleus (Fig. 5 *B–D*). These nuclei appear pycnotic, are often surrounded by a perinuclear vacuole, and stain TUNEL positive (Fig. 5*E*), suggesting that they are apoptotic. As the midgut is one of the primary organs responsible for osmoregulation, such systematic destruction of the midgut epithelium would be consistent with the loss of body turgor associated with the floppy phenotype.

In conclusion, the gene *mcf* encodes a novel high molecular weight toxin that destroys both the insect gut and insect hemocytes. As both affected tissues show clear signs of apoptosis, these data are consistent with the hypothesis that *mcf* encodes a novel BH3 containing pro-apoptotic toxin. Destruction of the

hemocytes during infection correlates with a failure to successfully encapsulate and clear Mcf expressing bacteria during infection. Destruction of the insect midgut, a primary organ in osmoregulation, is probably responsible for the marked loss of body turgor observed in the floppy phenotype. As both the hemocytes and the midgut are destroyed by injection of either *E. coli* expressing Mcf or by Mcf toxin itself, we can infer that Mcf interacts with, or is uptaken by, the hemocoel side of the insect midgut. However, the normal method of secretion of Mcf from *P. luminescens* itself, or its mode of action on insect cells, remains obscure. Finally, although there is considerable current interest in toxins which act on the insect gut, such as the δ-endotoxins from *Bacillus thuringiensis* (24) and the toxin complexes from *P. luminescens* (8), toxins, like Mcf, which act on both the gut and the insect immune system represent a promising, yet underexploited, avenue for future insecticide development.

We thank S. E. Reynolds for comments on the manuscript and help with hemocyte work, the laboratory of D. J. Clarke for useful input, and R. Adams for help with time-lapse photography. The plasmid *pBBR2-GFP* was a kind gift of L. Eberl. This work was supported by grants from the Biotechnology and Biological Sciences Research Council (Exploiting Genomics) and the Royal Society (Merit Award to R.ff.-C.) and by an exchange program between the United Kingdom and Brazil (CAPES to C.P.S.).

1. Razin, S., Yogev, D. & Naot, Y. (1998) *Microbiol. Mol. Biol. Rev.* **62,** 1094–1156.
2. Andersson, J. O. (2000) *Curr. Biol.* **10,** R866–R868.
3. Ochman, H. & Moran, N. A. (2001) *Science* **292,** 1096–1098.
4. Fitzgerald, J. R. & Musser, J. M. (2001) *Trends Microbiol.* **9,** 547–553.
5. Forst, S., Dowds, B., Boemare, N. & Stackebrandt, E. (1997) *Annu. Rev. Microbiol.* **51,** 47–72.
6. Forst, S. & Clarke, D. (2001) in *Entomopathogenic Nematology*, ed. Gaugler, R. (CAB International, London), pp. 57–77.
7. ffrench-Constant, R. H., Waterfield, N., Burland, V., Perna, N. T., Daborn, P. J., Bowen, D. & Blattner, F. R. (2000) *Appl. Environ. Microbiol.* **66,** 3310–3329.
8. Bowen, D., Rocheleau, T. A., Blackburn, M., Andreev, O., Golubeva, E., Bhartia, R. & ffrench-Constant, R. H. (1998) *Science* **280,** 2129–2132.
9. Forst, S. & Nealson, K. (1996) *Microbiol. Rev.* **60,** 21–43.
10. Waterfield, N. R., Bowen, D. J., Fetherston, J. D., Perry, R. D. & ffrench-Constant, R. H. (2001) *Trends Microbiol.* **9,** 185–191.
11. Silva, C. P., Waterfield, N. R., Daborn, P. J., Dean, P., Chilver, T., Au, C. P. Y., Sharma, S., Potter, U., Reynolds, S. E. & ffrench-Constant, R. H. (2002) *Cell. Microbiol.* **4,** 329–339.
12. Pech, L. L. & Strand, M. R. (1995) *J. Insect Physiol.* **41,** 481–488.
13. Pech, L. L. & Strand, M. R. (1996) *J. Cell Sci.* **109,** 2053–2060.
14. Budd, R. C. (2001) *Curr. Opin. Immunol.* **13,** 356–362.
15. Fischer-Le Saux, M., Viallard, V., Brunel, B., Normand, P. & Boemare, N. E. (1999) *Int. J. Syst. Bacteriol.* **49,** 1645–1646.
16. Blackburn, M., Golubeva, E., Bowen, D. & ffrench-Constant, R. H. (1998) *Appl. Environ. Microbiol.* **64,** 3036–3041.
17. Hofmann, F., Busch, C., Prepens, U., Just, I. & Aktories, K. (1997) *J. Biol. Chem.* **272,** 11074–11078.
18. Schaller, A., Kuhn, R., Kuhnert, P., Nicolet, J., Anderson, T. J., MacInnes, J. I., Segers, R. P. & Frey, J. (1999) *Microbiology* **145,** 2105–2116.
19. Christie, P. J. & Vogel, J. P. (2000) *Trends Microbiol.* **8,** 354–360.
20. Berger, K. H., Merriam, J. J. & Isberg, R. R. (1994) *Mol. Microbiol.* **14,** 809–822.
21. Stanley Samuelson, D. W., Jensen, E., Nickerson, K. W., Tiebel, K., Ogg, C. L. & Howard, R. W. (1991) *Proc. Natl. Acad. Sci. USA* **88,** 1064–1068.
22. Kravtsov, V. D., Daniel, T. O. & Koury, M. J. (1999) *Am. J. Pathol.* **155,** 1327–1339.
23. Rueckschloss, U. & Isenberg, G. (2001) *J. Physiol. (Cambridge)* **537,** 363–370.
24. Schnepf, E., Crickmore, N., Van Rie, J., Lereclus, D., Baum, J., Feitelson, J., Zeigler, D. R. & Dean, D. H. (1998) *Microbiol. Mol. Biol. Rev.* **62,** 775–806.